Dalton Transactions

Steric Control of Dioxygen Activation Pathways for MnII Complexes Supported by Pentadentate, Amide-containing Ligands

Journal:	*Dalton Transactions*
Manuscript ID	DT-ART-06-2019-002682.R1
Article Type:	Paper
Date Submitted by the Author:	23-Jul-2019
Complete List of Authors:	Parham, Joshua; University of Kansas Wijeratne, Gayan; University of Alabama at Birmingham College of Arts and Sciences, Chemistry Mayfield, Jaycee; University of Kansas Jackson, Timothy; University of Kansas

Steric Control of Dioxygen Activation Pathways for Mn^{II} Complexes Supported by Pentadentate, Amide-containing Ligands†

Joshua D. Parham‡, Gayan B. Wijeratne‡,⁑, Jaycee Mayfield‡ and Timothy A. Jackson‡*

‡*Department of Chemistry and Center for Environmentally Beneficial Catalysis, University of Kansas, Lawrence, Kansas 66045, United States*

⁑ Current Address: *Department of Chemistry, The University of Alabama at Birmingham, Birmingham, Alabama 35205, United States*

*To whom correspondence should be addressed:
Timothy A. Jackson
Phone: (785) 864-3968
taj@ku.edu

†Electronic supplementary information (ESI) available: Additional spectroscopic data for Mn intermediates, ^{1}H NMR analysis of organic oxidation products, DFT-optimized Cartesian coordinates.

Abstract.

Dioxygen activation at manganese centers is well known in nature, but synthetic manganese systems capable of utilizing O_2 as an oxidant are relatively uncommon. These present investigations probe the dioxygen activation pathways of two mononuclear Mn^{II} complexes supported by pentacoordinate amide-containing ligands, [Mn^{II}(dpaq)](OTf) and the sterically modified [Mn^{II}(dpaq^{2Me})](OTf). Dioxygen titration experiments demonstrate that [Mn^{II}(dpaq)](OTf) reacts with O_2 to form [Mn^{III}(OH)(dpaq)](OTf) according to a 4:1 Mn:O_2 stoichiometry. This stoichiometry is consistent with a pathway involving comproportionation between a Mn^{IV}-oxo species and residual Mn^{II} complex to form a (μ-oxo)dimanganese(III, III) species that is hydrolyzed by water to give the Mn^{III}-hydroxo product. In contrast, the sterically modified [Mn^{II}(dpaq^{2Me})](OTf) complex was found to react with O_2 according to a 2:1 Mn:O_2 stoichiometry. This stoichiometry is indicative of a pathway in which a Mn^{IV}-oxo intermediate abstracts a hydrogen atom from solvent instead of undergoing comproportionation with the Mn^{II} starting complex. Isotopic labeling experiments, in which the oxygenation of the Mn^{II} complexes was carried out in deuterated solvent, supported this change in pathway. The oxygenation of [Mn^{II}(dpaq)](OTf) did not result in any deuterium incorporation in the Mn^{III}-hydroxo product, while the oxygenation of [Mn^{II}(dpaq^{2Me})](OTf) in d_3-MeCN showed [Mn^{III}(OD)(dpaq^{2Me})]$^+$ formation. Taken together, these observations highlight the use of steric effects as a means to select which intermediates form along dioxygen activation pathways.

Introduction.

Dioxygen activation at metal centers is widespread in biology.[1-4] While Nature most commonly employs Fe- and Cu-containing enzymes for O_2 activation, there are examples of Mn enzymes that participate in these reactions.[3] Mn enzymes that require dioxygen for activity include manganese-dependent homoprotocatechuate 2,3-dioxygenase (HPCD),[5, 6] manganese lipoxygenase,[7-9] and the oxalate-degrading enzymes oxalate oxidase[10, 11] and oxalate decarboxylase.[12, 13] In a synthetic setting, the possibility of pairing an earth-abundant metal like Mn with an oxidant as benign and ubiquitous as O_2 is attractive, especially as industrial O_2 activation often employs expensive precious-metal catalysts.[14] However, examples of Mn^{II} complexes that can activate dioxygen to give isolable products are relatively uncommon. This lack of reactivity towards O_2 is due in part to the high reduction potential of the $Mn^{III/II}$ redox couple (1.5 V vs. NHE in H_2O).[15] To circumvent this shortcoming, electron-rich ligands have been used to modulate the reduction potential of the Mn^{II} center and therefore facilitate O_2 activation.[16] Systems employing these electron-rich ligand scaffolds perform catalytic dioxygen reduction and organic substrate oxidation using O_2.[17-25] The mechanistic details of many of these catalysts remain unclear, due in part to the fleeting nature of the intermediates along these reaction pathways.[16, 20, 23, 24]

An early example of O_2 as an oxidant for Mn-catalyzed substrate oxidation was reported by Fontecave and coworkers and utilized the Mn(TPP) system (TPP = tetraphenylporphyrin).[20] In the presence of O_2, 1-methylimidazole as a co-catalyst, and acetic acid as a proton source, the [Mn^{II}(TPP)] catalysts performed olefin epoxidation, with up to 75 turnovers.[20] Although impressive in coupling O_2 activation with substrate oxidation, the mechanistic details of this system are not well understood.

In one of the first reports to propose a mechanism of O_2 activation by a synthetic Mn complex, Horwitz described electrocatalytic olefin epoxidation using the [Mn^{II}(salen)] complex, which was generated electrochemically via reduction of [Mn^{III}(salen)]$^+$ (salen = *N*,*N*′-bis(salicylidene)ethylenediamine).[21] On the basis of cyclic voltammetry, the Mn^{II} species was proposed to bind dioxygen and, with the electrochemical transfer of a second electron, yield an η^2-peroxomanganese(III) complex. The putative [$Mn^{III}(O_2)$(salen)]$^-$ species was proposed to react with benzoic anhydride to form a high-valent Mn^{V}-oxo adduct that performed olefin epoxidation or allylic hydroxylation.[21] Work reported by Christoffers *et al.* using $Mn(OAc)_2 \bullet 4\ H_2O$ and O_2 to hydroxylate β-keto esters similarly invoked a Mn^{V}-oxo intermediate as the reactive species.[23]

There have also been a small number of Mn^{II} complexes that activate O_2 to form isolable, mid-valent Mn^{III} complexes, for which various O_2-activation pathways have been proposed (Scheme 1). [26-33] Borovik and co-workers described a Mn^{II} complex with trianionic N4 ligation that reacts with O_2 to form a monomeric Mn^{III}-hydroxo complex, with a Mn:O_2 stoichiometry of 2:1.[26] Isotopic labeling experiments with $^{18}O_2$ confirmed that the O atoms in the Mn^{III}-hydroxo product came solely from dioxygen. When this reaction was carried out in the presence of 1 equivalent of PPh_3, the oxygen atom transfer (OAT) product $Ph_3P{=}O$ was observed in 33% yield. Additionally, reactions in deuterated solvent yielded only the Mn^{III}–OD complex. These observations support a mechanism involving the initial formation of a peroxodimanganese(III, III) species from two equivalents of the Mn^{II} complex and O_2. This dimer was proposed to undergo homolytic O−O bond cleavage to yield two Mn^{IV}-oxo complexes that abstract hydrogen atoms from solvent to generate the observed Mn^{III}-hydroxo product (Scheme 1A).[26]

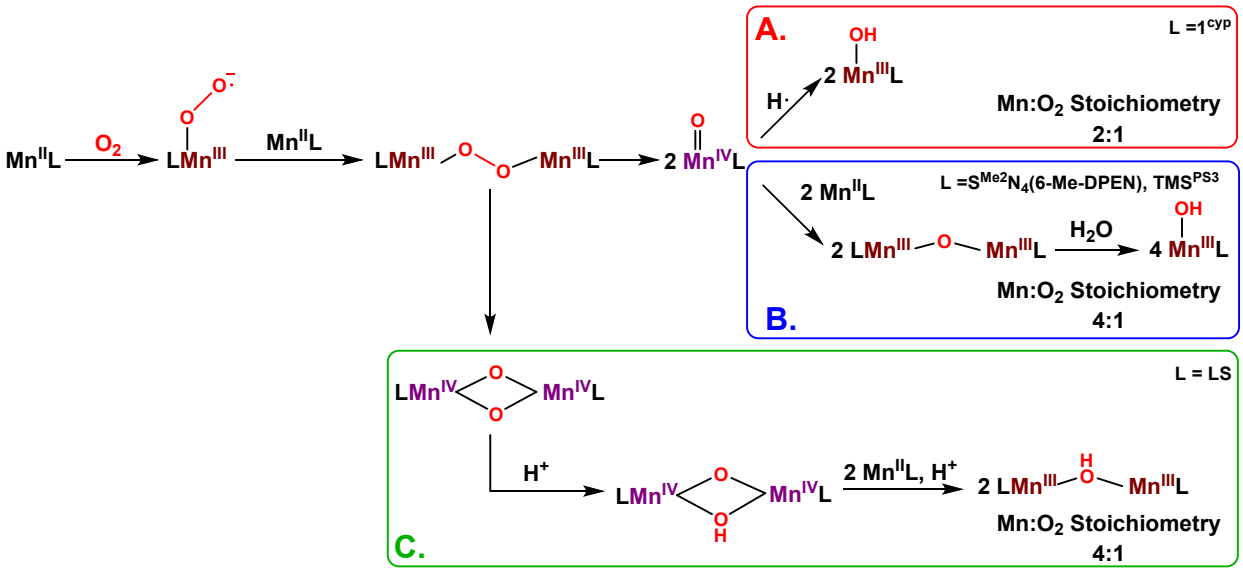

Scheme 1. Proposed mechanisms for the reaction of Mn^{II} complexes with O_2 to generate Mn^{III}-hydroxo species. Ligand abbreviations are as follows: 1^{cyp} = tris(N-cyclopentylcarbamoylmethyl)amine; $S^{Me2}N_4$(6-Me-DPEN) = (E)-3-((2-(bis((6-methylpyridin-2-yl)methyl)amino)ethyl)imino)-2-methylbutane-2-thiolate); TMS^{PS3} = (2,2′,2″-trimercapto-3,3′,3″-tris(trimethylsilyl)triphenylphosphine); LS = 2,2′-(2,2′-bipyridine-6,6′-diyl)bis(1,1′-diphenylethanethiolate).[18, 26-29, 31, 32]

More recently, Kovacs *et al.* reported a series of Mn^{II} complexes featuring N_4S^- ligation that also reacted with O_2 to give the corresponding mononuclear Mn^{III}-hydroxo complexes.[29] However, these systems operate with a Mn:O_2 stoichiometry of 4:1, differing from that of the Borovik system (2:1). An X-ray diffraction structure of $[Mn^{III}Mn^{III}(\mu\text{-}\eta^1\text{:}\eta^1\text{-}O_2)(S^{Me2}N_4(6\text{-Me-DPEN}))_2]^{2+}$ confirmed the initial formation of a peroxodimanganese(III, III) species from the reaction of two equivalents of the five-coordinate $[Mn^{II}(S^{Me2}N_4(6\text{-Me-DPEN}))]^+$ complex with O_2 ($S^{Me2}N_4$(6-Me-DPEN)) = (E)-3-((2-(bis((6-methylpyridin-2-yl)methyl)amino)ethyl)imino)-2-methylbutane-2-thiolate). The decay of $[Mn^{III}Mn^{III}(\mu\text{-}\eta^1\text{:}\eta^1\text{-}O_2)(S^{Me2}N_4(6\text{-Me-DPEN}))_2]^{2+}$ yielded the (μ-oxo)dimanganese(III, III) species $[Mn^{III}Mn^{III}(\mu\text{-O})(S^{Me2}N_4(6\text{-Me-DPEN}))_2]^{2+}$, which can undergo hydrolysis to generate the Mn^{III}-hydroxo complex (Scheme 1B).[18, 27, 29] The formation of the (μ-oxo)dimanganese(III, III) species, which was also characterized by X-ray diffraction, suggests a

mechanism where a Mn^{IV}-oxo adduct (or a bis(μ-oxo)dimanganese(IV, IV) dimer) is intercepted by unreacted Mn^{II} complex, rather than abstracting a hydrogen atom from solvent.[32]

A similar mechanism was invoked by Lee *et al.* for O_2 activation by the $[Mn(^{TMS}PS3)(DABCO)]^-$ system ($^{TMS}PS3$ = (2,2′,2″-trimercapto-3,3′,3″-tris(trimethylsilyl)triphenylphosphine) and DABCO = 1,4- diazabicyclo[2.2.2]octane).[31] In this work, a crystallographically characterized monomeric side-on Mn^{IV}-peroxo species is formed from the reaction of $[Mn(^{TMS}PS3)(DABCO)]^-$ with O_2. This species is able to react with additional $[Mn(^{TMS}PS3)(DABCO)]^-$, leading to the formation of a putative peroxodimanganese(III, III) species that is proposed to decay and form either a terminal Mn^{IV}-oxo or a bis(μ-oxo)dimanganese(IV, IV) intermediate. This intermediate undergoes a subsequent comproportionation with residual Mn^{II} complex in solution to form a (μ-oxo)dimanganese(III, III) species.[31, 33]

A subtly different mechanism of O_2 activation, by a dimercapto-bridged Mn^{II} dimer, was recently proposed by Duboc *et al.*[28, 30] In this system, O_2 activation resulted in the production of a (μ-hydroxo)dimanganese(III, III) complex, which was characterized crystallographically. The initial formation of a peroxodimanganese(III, III) intermediate was proposed from the reaction of the Mn^{II} dimer with O_2. However, instead of yielding terminal Mn^{IV}-oxo species upon homolytic O−O bond cleavage, the peroxo-bridged dimer was proposed to convert to a bis(μ-oxo)dimanganese(IV, IV) intermediate, which was crystallographically characterized. The bis(μ-oxo)dimanganese(IV, IV) complex then decayed by an intramolecular proton transfer between the supporting ligand and one of the bridging oxo atoms to give a (μ-oxo)(μ-hydroxo)dimanganese(IV, IV) species. Finally, the (μ-oxo)(μ-hydroxo)dimanganese(IV, IV) species was proposed to

comproportionate with residual Mn^{II} dimer to give the final (μ-hydroxo)dimanganese(III, III) product (Scheme 1C).[28, 30]

Collectively, these reports highlight some central features in O_2 activation by Mn^{II} centers. In all cases, a μ-peroxodimanganese(III, III) species is invoked as an early intermediate, and this species decays by O–O homolysis to give either mononuclear Mn^{IV}-oxo or dinuclear bis(μ-oxo)dimanganese(IV, IV) intermediates. At this point, the paths diverge (Scheme 1), but isolable Mn^{III} complexes are the products of all pathways, and trapping of high-valent Mn^{IV} species by reaction with the Mn^{II} starting complex is common. Importantly, in no pathway is the starting Mn^{II} complex regenerated.

As part of our on-going efforts to mimic the chemistry of Mn-dependent enzymes,[34, 35] we have previously reported a pair of Mn^{II} complexes supported by amide-containing N_5 ligands, $[Mn^{II}(dpaq)](OTf)$ and $[Mn^{II}(dpaq^{2Me})](OTf)$, that react with O_2 to yield the corresponding Mn^{III}-hydroxo adducts, $[Mn^{III}(OH)(dpaq)]^+$ and $[Mn^{III}(OH)(dpaq^{2Me})]^+$, in 98% yield (Scheme 2, dpaq = 2-[bis(pyridin-2-ylmethyl)]amino-N-quinolin-8-yl-acetamidate and $dpaq^{2Me}$ = 2-[bis(pyridin-2-ylmethyl)]amino-N-2-methyl-quinolin-8-yl-acetamidate). These Mn^{III}-hydroxide complexes can oxidize 2,2′-6,6′-tetramethylpiperidine-1-ol (TEMPOH), phenols, and xanthene through a hydrogen-atom transfer (HAT) mechanism.[19, 36, 37] However, the pathway by which $[Mn^{II}(dpaq)](OTf)$ and $[Mn^{II}(dpaq^{2Me})](OTf)$ react with dioxygen has not been explored. A recent report has shown that, upon dissolution of the $[Mn^{III}(OH)(dpaq)](OTf)$ salt in MeCN solution, the mononuclear Mn^{III}-hydroxo adduct exists in a water-dependent equilibrium with a (μ-oxo)dimanganese(III, III) species (Scheme 2, top).[37] Using ^{1}H-NMR and electronic absorption spectroscopies, we demonstrated that the addition of a small amount of water (440 equivalents per Mn^{III}) to an equilibrium mixture of $[Mn^{III}(OH)(dpaq)]^+$ and $[Mn^{III}Mn^{III}(\mu\text{-oxo})(dpaq)_2]^{2+}$ shifts the

equilibrium to favor the mononuclear Mn^{III}-hydroxo species.[37] This equilibrium has also been observed for complexes featuring different substituents in the 5-quinolinyl position of the dpaq ligand ($[Mn^{III}(OH)(dpaq^{5Cl})_2](OTf)$, $[Mn^{III}(OH)(dpaq^{5OMe})_2](OTf)$, and $[Mn^{III}(OH)(dpaq^{5NO2})_2](OTf)$), and we have obtained XRD structures of each of the respective $[Mn^{III}Mn^{III}(\mu\text{-}O)(dpaq^{5R})_2](OTf)_2$ complexes (R = Cl, OMe, and NO_2).[38] The observation of the (μ-oxo)dimanganese(III, III) complexes could be taken to suggest that the $[Mn^{II}(dpaq^{5R})](OTf)$ complexes carry out O_2 activation in a manner similar to that observed for the $[Mn^{II}(S^{Me2}N_4(6\text{-Me-DPEN}))]^+$ complex of Kovacs and co-workers (Scheme 1B).[29] Intriguingly, complementary ^{1}H-NMR investigations studies of $[Mn^{II}(dpaq^{2Me})](OTf)$ provided no evidence for a (μ-oxo)dimanganese(III, III) species (Scheme 2, bottom).[37] Presumably, the steric bulk of the 2-Me-appended quinoline moiety in $dpaq^{2Me}$ disfavors the formation of an oxo-bridged dimer.

In this study, we have performed O_2 titrations, substrate trapping experiments, and isotopic labeling studies to evaluate the O_2 activation mechanisms of the $[Mn^{II}(dpaq)](OTf)$ and $[Mn^{II}(dpaq^{2Me})](OTf)$ complexes. The O_2 titrations revealed that dioxygen activation by $[Mn^{II}(dpaq)](OTf)$ and $[Mn^{II}(dpaq^{2Me})](OTf)$ proceed with different Mn:O_2 stoichiometries. Specifically, $[Mn^{II}(dpaq)](OTf)$ operates according to a Mn:O_2 stoichiometry of 4:1 while $[Mn^{II}(dpaq^{2Me})]^+$ operates with a Mn:O_2 stoichiometry of 2:1. Dioxygen activation experiments for $[Mn^{II}(dpaq)](OTf)$ in deuterated solvent showed complete formation of the unlabeled Mn^{III}–OH product, suggesting that hydrogen-atom abstraction from solvent is not involved in the O_2-activation pathway of this complex. In contrast, when the $[Mn^{II}(dpaq^{2Me})](OTf)$ complex, which features a bulkier supporting ligand, was treated with dioxygen in deuterated solvent, we observed the Mn^{III}–OD product, indicative of an alternative dioxygen-activation pathway involving hydrogen-atom abstraction from solvent. These results demonstrate that subtle changes

in the steric properties of the supporting ligand can greatly influence the O_2 activation pathway of Mn^{II} complexes.

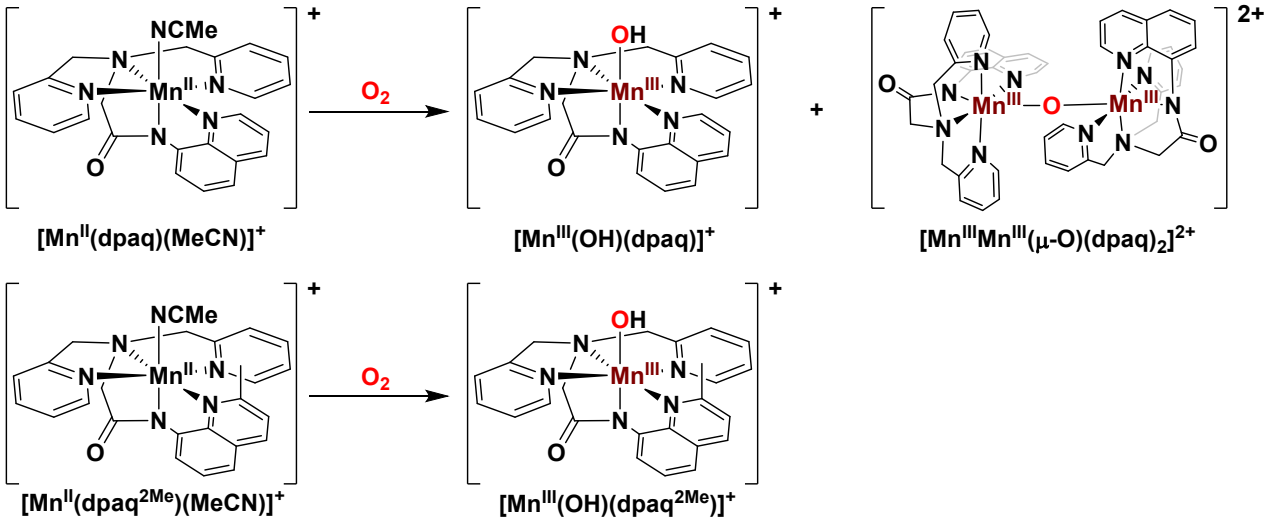

Scheme 2. $[Mn^{II}(dpaq)(MeCN)]^+$ reacts with O_2 to produce a mixture of (μ-oxo)dimanganese(III, III) and monomeric $[Mn^{III}(OH)(dpaq)]^+$ species (top). $[Mn^{II}(dpaq^{2Me})(MeCN)]^+$ does not show formation of a (μ-oxo)dimanganese(III, III) complex in the reaction with O_2, instead only forming $[Mn^{III}(OH)(dpaq^{2Me})]^+$ (bottom).

Experimental.

Materials and Instrumentation. All chemicals were used as obtained from commercial sources unless noted otherwise. Acetonitrile and diethyl ether were dried and degassed using a PureSolv Micro solvent purification system. This drying procedure results in MeCN that, on average, contains 64(8) ppm (or 3.6 mM) H_2O.[37] The O_2 gas used was >99% pure and further purified by passing through a column packed with drierite and 5 Å molecular sieves. $[Mn^{II}(dpaq)](OTf)$ and $[Mn^{II}(dpaq^{2Me})](OTf)$ were synthesized and characterized as reported previously.[19, 36] Deuterated acetonitrile was dried over 3 Å molecular sieves. Electronic absorption experiments were performed using a Varian Cary 50 Bio UV-Visible spectrophotometer. Electrospray ionization-mass spectrometry (ESI-MS) experiments were performed using an LCT Premier MicroMass electrospray time-of-flight instrument. ^1H and ^{31}P NMR spectra were obtained on a Bruker DRX

400 MHz NMR spectrometer. Gas chromatography-mass spectrometry (GC-MS) experiments were performed with a Quattro Micro GC quadrupole mass analyzer via an Agilent 6890 N gas chromatograph.

Determination of manganese:oxidant stoichiometry in Mn^{III}-hydroxo formation from [Mn^{II}(dpaq)](OTf) or [Mn^{II}($dpaq^{2Me}$)](OTf) and O_2. Solutions of [Mn^{II}(dpaq)](OTf) or [Mn^{II}($dpaq^{2Me}$)](OTf) (6 mM in MeCN) were prepared under an argon atmosphere in a glove box. The solutions were sealed in quartz cuvettes with pierceable septa. In a separate vial, dried MeCN was saturated with O_2 by bubbling the gas through the solvent after running the gas through a 20 cm column packed with drierite and 5 Å molecular sieves. The concentration of O_2 in saturated MeCN is known to be 8.1 mM at 25˚C.[39] Although the O_2 was passed through drying materials, this procedure did not remove all the H_2O. Karl-Fischer titrations of a 4 mL MeCN solution with a Mettler Toledo DL39 coulometric titrator of a MeCN solution following a 30 minute O_2 purge showed a water content of 2352(4) ppm (or 131 mM), an increase of 368% relative to dried MeCN. Measured amounts of saturated solvent were added to the solutions of [Mn^{II}(dpaq)](OTf) or [Mn^{II}($dpaq^{2Me}$)](OTf) using gastight syringes to deliver 0.1, 0.18, 0.25, 0.5, or 1 equivalents of O_2 relative to Mn^{II} concentration. This procedure resulted in the concomitant addition of 0.1 – 1 equivalents of H_2O relative to the Mn concentration . Additionally, 400 equivalents of H_2O were added to the solutions of [Mn^{II}(dpaq)](OTf) to ensure formation of the monomeric [Mn^{III}(OH)(dpaq)]$^+$ product.[37] The reactions were monitored by electronic absorption spectroscopy at 25˚C until the spectra ceased to change (typically ~4 hours). The percent formation of [Mn^{III}(OH)(dpaq)]$^+$ or [Mn^{III}(OH)($dpaq^{2Me}$)]$^+$ was determined by exposing the reaction mixtures to additional O_2 (i.e., opening the solutions to atmosphere) until full formation of the Mn^{III}-hydroxide species was achieved (~18 hours), upon which absorption spectra were

obtained and compared to those obtained from the titrations. Each measurement was performed in triplicate.

Reactions between [Mn^{II}(dpaq)](OTf) or [Mn^{II}($dpaq^{2Me}$)](OTf) and O_2 in deuterated solvent. 6 mM solutions of [Mn^{II}(dpaq)](OTf) or [Mn^{II}($dpaq^{2Me}$)](OTf) in deuterated d_3-MeCN were prepared under an inert atmosphere in a glove box. The solutions were sealed in vials with pierceable septa. 1 equivalent of O_2 was added to the solution via the addition of measured amounts of saturated solvent with a gas-tight syringe. The reactions were allowed to stir overnight, and the resulting solutions were analyzed by ESI-MS.

Reactions between [Mn^{II}(dpaq)](OTf) or [Mn^{II}($dpaq^{2Me}$)](OTf) and O_2 in the presence of PPh_3. 6 mM solutions of [Mn^{II}($dpaq^{2Me}$)](OTf) with 50 equivalents of PPh_3 in d_3-MeCN were prepared in vials sealed by pierceable septa. Excess O_2 gas was added via syringe, and the reactions were allowed to stir for 3 hours at 25˚C. Following the reactions, the solvent was removed and the organic products were dissolved in diethyl ether. The colorless solution was filtered through a syringe filter. Product analysis was performed by GC-MS and ^{31}P NMR, and signals were compared to authentic samples of PPh_3 and O=PPh_3.

Reactions between [Mn^{II}(dpaq)](OTf) or [Mn^{II}($dpaq^{2Me}$)](OTf) and O_2 in the presence of hydrocarbon substrates. 6 mM solutions of [Mn^{II}(dpaq)](OTf) or [Mn^{II}($dpaq^{2Me}$)](OTf) with 250 equivalents of cyclohexane, *cis*-dimethylcylohexane, cyclooctane, or ethylbenzene in d_3-MeCN were prepared and sealed in vials with pierceable septa. Reactions exploring the oxidation of toluene were carried out in a 1:1 mixture of toluene and d_3-MeCN. Excess O_2 gas was introduced to each solution via syringe, and the reactions were allowed to stir for 3 hours at 25˚C. Following the reaction, the solutions were passed through a silica plug and eluted with 2 mL of d_3-MeCN or

deuterated chloroform. Product analysis was performed by ^{1}H-NMR using naphthalene as an internal standard.

The oxidation of 9,10-dihydroanthracene (DHA) was performed in a similar manner by preparing 6 mM solutions of [Mn^{II}(dpaq)](OTf) or [Mn^{II}(dpaq^{2Me})](OTf) in d_3-MeCN and adding 100 equivalents of DHA that had been dissolved in the minimal amount of dichloromethane. The vials were sealed with pierceable septa, excess O_2 was added via syringe, and the reactions were allowed to stir for three hours. The reaction mixtures were passed through silica plugs and eluted with dichloromethane. The solvent was removed and product analysis was performed by ^{1}H NMR spectroscopy in $CDCl_3$ with 1,4-benzoquinone as a quantitative reference. ESI-MS experiments were also performed following a reaction between [Mn^{II}(dpaq)](OTf) or [Mn^{II}(dpaq^{2Me})](OTf) and DHA in the presence of 1 equivalent of O_2 (delivered via saturated solvent in a gas-tight syringe) in d_3-MeCN.

Reactions between [Mn^{III}(OH)(dpaq)](OTf) or [Mn^{III}(OH)(dpaq^{2Me})](OTf) and 9,10-dihydroanthracene in the absence of O_2. 6 mM solutions of [Mn^{II}(dpaq)](OTf) or [Mn^{II}(dpaq^{2Me})](OTf) in d_3-MeCN were prepared under inert atmosphere in vials sealed with pierceable septa, and 100 equivalents of DHA that had been dissolved in the minimal amount of dichloromethane was added. The reactions were allowed to stir for three hours. The reaction mixtures were passed through silica plugs and eluted with dichloromethane. The solvent was removed and product analysis was performed by ^{1}H NMR spectroscopy in $CDCl_3$ with 1,4-benzoquinone as a quantitative reference.

Computational studies to investigate the energetics of μ-oxodimanganese(III,III) formation. The *ORCA* 4.0.1 software package was used to perform all DFT calculations. Geometry optimizations and numerical frequency calculations utilized the BP86 functional[40, 41] with the RI

approximation[42] and def2-J auxiliary basis set.[43] Single point calculations were performed using the B3LYP functional,[44-46] utilizing the RIJCOSX approximation,[47, 48] and def2-J auxiliary basis set. Both the BP86 and B3LYP computations employed the def2-SVP basis set for C and H atoms and the def2-TZVP basis set for Mn, O, and N.[49-51] The broken symmetry method was used to properly describe the effects of antiferromagnetic coupling for the $S = 0$ $[Mn^{III}Mn^{III}(\mu\text{-}O)(dpaq^{R})_2]^{2+}$ complexes.[52-54] The conductor-like polarizable continuum (CPCM) solvent model (for acetonitrile)[55, 56] was used for all calculations for Mn^{IV}-oxo and Mn^{II}-solvento complexes and MeCN, as well as for single point calculations of $[Mn^{III}Mn^{III}(\mu\text{-}O)(dpaq^{R})_2]^{2+}$. All numerical frequency calculations showed no imaginary frequencies, confirming that the optimized structures are representative of the minimum energy geometries. Utilizing a solvent model in conjunction with the broken symmetry method resulted in difficulties completing the numerical frequency calculations for the dimer species. For this reason, the solvent model was neglected in geometry optimizations and frequency calculations for $[Mn^{III}Mn^{III}(\mu\text{-}O)(dpaq^{R})_2]^{2+}$ but was included in single point energy calculations. In order to investigate the effects of neglecting solvation for the geometry optimization procedure, we performed geometry optimizations of $[Mn^{IV}(O)(dpaq^{H})]^{+}$ and $[Mn^{III}Mn^{III}(\mu\text{-}O)(dpaq^{H})_2]^{2+}$ with and without the inclusion of a CPCM for solvation. We then compared the single point energies, which included the use of CPCM, for these different structures. In both cases, the energies of the models developed using solvation were less than 1 kcal/mol higher than the energies of the models developed lacking solvation. Thus, it was determined that geometry optimizations and numerical frequency calculations for $[Mn^{III}Mn^{III}(\mu\text{-}O)(dpaq^{R})_2]^{2+}$ could be performed without the solvent model with no major impact on the final single point energy (Table S2).

Single point energies of DFT-optimized Mn^{IV}-oxo and Mn^{II}-solvento complexes were calculated and summed to determine the reactant energy. For the energy of products, similar calculations were done for a pairing of a single MeCN molecule and the (μ-oxo)dimanganese(III, III) complexes. The difference between the reactant and product energies were compared between complexes of the dpaq and $dpaq^{2Me}$ systems.

Results and Analysis.

Formation of $[Mn^{III}(OH)(dpaq)](OTf)$ from the reaction of $[Mn^{II}(dpaq)](OTf)$ with O_2. Titration experiments were performed to determine the Mn:O_2 stoichiometry for the reaction of $[Mn^{II}(dpaq)](OTf)$ and O_2 to generate the $[Mn^{III}(OH)(dpaq)](OTf)$ complex. A potential complication in these experiments is the equilibrium between $[Mn^{III}(OH)(dpaq)](OTf)$ and $[Mn^{III}Mn^{III}(\mu\text{-}O)(dpaq)_2]^{2+}$ (Scheme 2).[37] We addressed this complication by adding 400 equivalents of N_2-sparged H_2O to each sample, based on previous investigations that demonstrated that the addition of 400 equivalents of water caused the equilibrium to shift such that $[Mn^{III}(OH)(dpaq)](OTf)$ is the only species observed by ^{1}H-NMR spectroscopy.[37]

As the concentration of O_2 in saturated MeCN is known (8.1 mM at 25˚C),[39] the addition of O_2-saturated solvent is a convenient method for accurate O_2 delivery. Aliquots of MeCN solutions containing 0.1, 0.18, 0.25, 0.5, and 1 equivalents of O_2 were added to $[Mn^{II}(dpaq)](OTf)$. The percent formation of $[Mn^{III}(OH)(dpaq)](OTf)$ from these experiments is shown in Figure 1 and Table 1 (overlay of the electronic absorption spectra collected for each aliquot is shown in Figure S1). From these data, it is evident that complete formation of $[Mn^{III}(OH)(dpaq)](OTf)$ is accomplished with ≥ 0.25 equivalents of O_2 (Figure 1, blue markers), giving a 4:1 manganese:dioxygen stoichiometry.

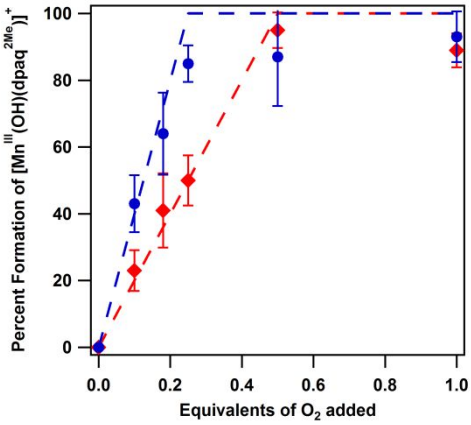

Figure 1. Plot of percent conversion to [Mn^{III}(OH)(dpaq)](OTf) (blue markers) and [Mn^{III}(OH)($dpaq^{2Me}$)](OTf) (red markers) as a function of added O_2. Error bars represent one standard deviation from the average of measurements performed in triplicate. Trend lines for 4:1 (blue dashes) and 2:1 (red dashes) Mn:O_2 stoichiometry are shown for comparison.

Table 1. Percent Conversion to Mn^{III}-hydroxo Adducts [Mn^{III}(OH)(dpaq)](OTf) and [Mn^{III}(OH)($dpaq^{2Me}$)](OTf) Compared to Expected Yields for 4:1 and 2:1 Mn:O_2 Stoichiometry.

Equivalents of O_2 added	Experimental % conversion to [Mn^{III}(OH)(dpaq)](OTf)	Experimental % conversion to [Mn^{III}(OH)($dpaq^{2Me}$)](OTf)	Theoretical yield	
			Mn:O_2 4:1	Mn:O_2 2:1
0	0	0	0	0
0.1	43±9	23±6	40	20
0.18	64±12	41±11	72	36
0.25	85±6	50±8	100	50
0.5	87±15	95±5	100	100
1.0	93±8	89±5	100	100

To assess the involvement of solvent in the formation of [Mn^{III}(OH)(dpaq)](OTf) from the reaction of [Mn^{II}(dpaq)](OTf) with O_2, we carried out the oxygenation reaction in deuterated d_3-MeCN. We observed no change in the apparent rate of formation of [Mn^{III}(OH)(dpaq)](OTf) in d_3-MeCN (Figure S2), and an ESI-MS analysis of the solution following the reaction showed only the presence of non-deuterated [Mn^{III}(OH)(dpaq)](OTf) (*m/z* = 454.1086, calculated *m/z* = 454.11, Figure 2A). An additional low-intensity peak around 455.11 *m/z* arises from the natural isotopic splitting of the compound, as illustrated by the mass spectrum of crystalline

[Mn^{III}(OH)(dpaq)](OTf) dissolved in d_3-MeCN (Figure 2B). Thus, we observe no evidence that the formation of [Mn^{III}(OH)(dpaq)](OTf) involves a HAT reaction with the solvent as the hydrogen-atom donor.

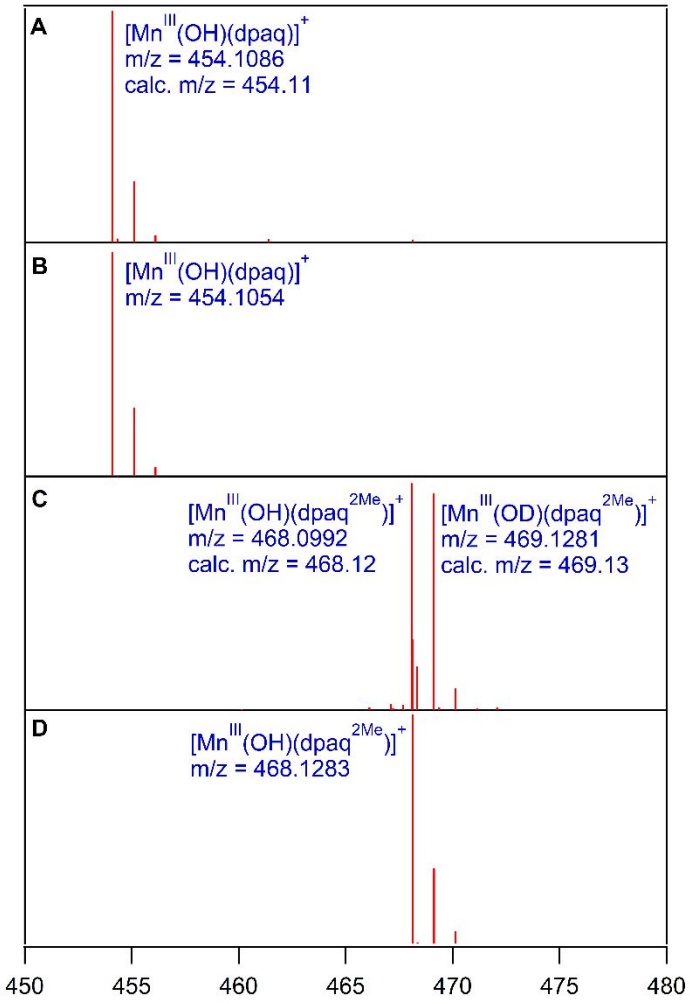

Figure 2. (A) ESI-MS data of $[Mn^{III}(OH)(dpaq)]^+$ from the reaction of [Mn^{II}(dpaq)](OTf) with O_2 in deuterated MeCN. (B) ESI-MS data of [Mn^{III}(OH)(dpaq)](OTf) dissolved in deuterated MeCN. (C) ESI-MS data for $[Mn^{III}(OD)(dpaq^{2Me})]^+$ and $[Mn^{III}(OH)(dpaq^{2Me})]^+$ from the reaction of [Mn^{II}($dpaq^{2Me}$)](OTf) with O_2 in deuterated MeCN. (D) ESI-MS data for [Mn^{III}(OH)($dpaq^{2Me}$)](OTf) dissolved in deuterated MeCN.

As the 4:1 manganese:dioxygen stoichiometry in the reaction of [Mn^{II}(dpaq)](OTf) with O_2 could indicate the involvement of a transient Mn^{IV}-oxo species (Scheme 1B), we attempted to trap this putative intermediate by carrying out the oxygenation of [Mn^{II}(dpaq)](OTf) in the presence of

PPh_3, a substrate known to react with Mn^{IV}-oxo adducts.[26, 57-59] In a typical reaction, $[Mn^{II}(dpaq)](OTf)$ was treated with an excess of O_2 in the presence of 50 equivalents of PPh_3 in d_3-MeCN. GC-MS experiments showed no evidence for the formation of the expected product of oxygen-atom transfer to PPh_3, triphenylphosphine oxide.

We also attempted to trap a putative Mn^{IV}-oxo intermediate by performing the oxygenation of $[Mn^{II}(dpaq)](OTf)$ in the presence of various hydrocarbons, which can react with a putative Mn^{IV}-oxo intermediate by a hydrogen-atom transfer mechanism.[58-64] For these experiments, $[Mn^{II}(dpaq)](OTf)$ was incubated with an excess of O_2 in the presence of 250 equivalents of the substrates in deuterated MeCN for 3hours. Oxygenation experiments in the presence of cyclohexane, *cis*-dimethylcylohexane, cyclooctane, toluene, and ethylbenzene resulted in no detection of oxidized organic products. When 100 equivalents of DHA, which has the weakest C–H bond dissociation free energy of this series, was used as the substrate, the formation of 3 equivalents of anthracene, 13 equivalents of anthrone, 2 equivalents of anthraquinone, and 8 equivalents of 9,10-dihydroanthracen-9-ol was observed by ^{1}H NMR spectroscopy (Figure S3). In total, 26 equivalents of DHA were consumed during the oxygenation reaction (Table S1). Control experiments in which d_3-MeCN solutions of DHA were stirred with excess O_2 in the absence of Mn^{II} complex did not yield any oxidized products. However, control experiments where $[Mn^{III}(OH)(dpaq)]^+$ was treated with 100 equivalents DHA in d_3-MeCN in the presence of O_2 revealed comparable formation of oxidized products (see Table S1), corresponding to the consumption of 30 equivalents of DHA. Accordingly, the DHA oxidation observed upon oxygenation of $[Mn^{II}(dpaq)](OTf)$ does not necessarily provide evidence for the formation of a Mn^{IV}-oxo intermediate. Instead, reaction of DHA with the Mn^{III}-hydroxo product, which can be regenerated by O_2 oxidation of $[Mn^{II}(dpaq)]^+$, could account for the observed DHA oxidation.

Formation of [Mn^{III}(OH)(dpaq^{2Me})](OTf) from the reaction of [Mn^{II}(dpaq^{2Me})](OTf) with O_2. We have previously noted that oxygenation of [Mn^{II}(dpaq^{2Me})](OTf) is substantially slower than that of [Mn^{II}(dpaq)](OTf),[36] and ^{1}H-NMR investigations of [Mn^{III}(OH)(dpaq^{2Me})](OTf) show no signals associated with a (μ-oxo)dimanganese(III, III) species, suggesting that this dimeric species is disfavored due to the bulk of the dpaq^{2Me} ligand.[37] As such, dioxygen titration experiments were performed for solutions of [Mn^{II}(dpaq^{2Me})](OTf) to investigate the effect of the steric bulk imposed by the methyl-quinoline group on this process. Similar to the experiments investigating the dioxygen reactivity of [Mn^{II}(dpaq)](OTf), aliquots of MeCN solutions containing 0.1, 0.18, 0.25, 0.5, and 1 equivalents of O_2 were added to [Mn^{II}(dpaq^{2Me})](OTf). The percent formation of [Mn^{III}(OH)(dpaq^{2Me})](OTf) from these experiments is shown in Figure 1 and Table 1 (overlay of the electronic absorption spectra collected for each aliquot is shown in Figure S4). In contrast to what is observed for [Mn^{II}(dpaq)](OTf), full formation of [Mn^{III}(OH)(dpaq^{2Me})](OTf) requires the addition of 0.5 equivalents of O_2 to a solution of [Mn^{II}(dpaq^{2Me})](OTf), suggesting a different reaction pathway (Figure 1 and Scheme 1A).

To further investigate the difference in mechanism observed for [Mn^{II}(dpaq^{2Me})](OTf), we performed the oxygenation reaction in d_3-MeCN. As is the case for [Mn^{II}(dpaq)](OTf), we observed no change in the apparent rate of formation of [Mn^{III}(OH)(dpaq^{2Me})](OTf) in d_3-MeCN (Figure S5). However, an ESI-MS analysis of the product solution revealed signals at *m*/*z* of 468.0992 and 469.1281, corresponding to [Mn^{III}(OH)(dpaq^{2Me})](OTf) and [Mn^{III}(OD)(dpaq^{2Me})](OTf), respectively, of nearly equal intensity (Figure 2C). A control experiment of [Mn^{III}(OH)(dpaq^{2Me})](OTf) dissolved in d_3-MeCN showed no ESI-MS signals associated with [Mn^{III}(OD)(dpaq^{2Me})](OTf) (Figure 2D). The low-intensity peak around 469.13 *m/z* arises from the natural isotopic splitting of the compound. Together, these observations suggest

that the deuterium incorporation for $[Mn^{III}(OD)(dpaq^{2Me})](OTf)$ arises from a hydrogen-atom abstraction from d_3-MeCN, although not during the rate determining step of the reaction. The observation of a mixture of $[Mn^{III}(OH)(dpaq^{2Me})](OTf)$ and $[Mn^{III}(OD)(dpaq^{2Me})](OTf)$ could arise from ligand substitution, where a portion of the OD^- ligands in $[Mn^{III}(OD)(dpaq^{2Me})](OTf)$ are substituted by OH^- from adventitious water present in the MeCN solution.

Substrate trapping experiments aimed to probe the formation of a Mn^{IV}-oxo intermediate upon oxygenation of $[Mn^{II}(dpaq^{2Me})](OTf)$ produced similar results to that seen for $[Mn^{II}(dpaq)](OTf)$. Oxygenation of $[Mn^{II}(dpaq^{2Me})](OTf)$ in the presence of 50 equivalents of PPh_3 failed to yield any observable oxidized products. Oxygenation experiments in the presence of cyclohexane, *cis*-dimethylcylohexane, cyclooctane, toluene, and ethylbenzene likewise resulted in no detection of oxidized organic products. Oxygenation of $[Mn^{II}(dpaq^{2Me})](OTf)$ in the presence of DHA yielded 3 equivalents of anthracene, 11.5 equivalents of anthrone, 7.5 equivalents of 9,10-dihydroanthran-9-ol, and 1.6 equivalents of anthraquinone (Figure S6). These amounts correspond to ca. 24 equivalents of DHA consumption during oxygenation (Table S1). An ESI-MS examination of a representative solution following the reaction of $[Mn^{II}(dpaq)]^+$ with O_2 in the presence of DHA showed no deuterium incorporation into the Mn^{III}-hydroxo product, indicating that the proton of the hydroxo ligand is not derived from a solvent molecule under these conditions (Figure S7). When a control experiment using $[Mn^{III}(OH)(dpaq^{2Me})](OTf)$ was performed, comparable product formation, corresponding to 34 equivalents of DHA consumed, was observed (Table S1). Presumably, the reaction between $[Mn^{III}(OH)(dpaq^{2Me})]^+$ and DHA results in the formation of a Mn^{II}-aqua complex that can react with excess O_2 and regenerate the Mn^{III}-hydroxo species.

Comparison of Formation Energies for (μ-oxo)dimanganese(III, III) Species. To better understand the basis for the apparent difference in O_2-activation pathways for $[Mn^{II}(dpaq)](OTf)$

and $[Mn^{II}(dpaq^{2Me})](OTf)$, DFT computations were performed to compare the energies of $[Mn^{III}Mn^{III}(\mu\text{-}O)(dpaq^{R})_2]^{2+}$ formation for these complexes. For these calculations, we assume that $[Mn^{III}Mn^{III}(\mu\text{-}O)(dpaq^{R})_2]^{2+}$ formation is achieved by reaction of the $[Mn^{IV}(O)(dpaq^{R})]^{+}$ and $[Mn^{II}(dpaq^{R})(NCMe)]^{+}$ complexes to give the $[Mn^{III}Mn^{III}(\mu\text{-}O)(dpaq^{R})_2]^{2+}$ product and acetonitrile. We compared the energetics of the reactions for the two ligand systems (dpaq and $dpaq^{2Me}$) by calculating the single-point energies of the reactants and products at infinite separation (we assume that the entropies of reaction will be similar for these systems).

To ensure that our computational protocol is reasonable, comparisons can be made between the structural parameters obtained from the DFT-optimized structure of $[Mn^{III}Mn^{III}(\mu\text{-}O)(dpaq)_2]^{2+}$ to those obtained from XRD data collected for previously characterized complexes of $[Mn^{III}Mn^{III}(\mu\text{-}O)(dpaq^{5R})_2]^{2+}$ (R=OMe, Cl, NO_2).[38] These derivatives feature a substitution at the 5-position of the quinoline unit on each ligand, introducing electronic effects without any steric interference on the bridging oxo site. The Mn–O bond of $[Mn^{III}Mn^{III}(\mu\text{-}O)(dpaq)_2]^{2+}$ is calculated to be slightly elongated with respect to the distances observed for the $dpaq^{5R}$ derivatives (1.810 Å versus 1.792-1.797 Å). When comparing the average Mn–N_{eq} bond distance, modest differences are seen between DFT and XRD structures, with $[Mn^{III}Mn^{III}(\mu\text{-}O)(dpaq)_2]^{2+}$ exhibiting an average bond length 0.055 - 0.062 Å longer. However, the Mn-N_{ax} distance for $[Mn^{III}Mn^{III}(\mu\text{-}O)(dpaq)_2]^{2+}$ (1.981 Å) falls within the range of distances observed for the $dpaq^{5R}$ derivatives (1.973 - 1.985 Å). Additionally, the calculated Mn–O–Mn bond angle of $[Mn^{III}Mn^{III}(\mu\text{-}O)(dpaq)_2]^{2+}$ exhibits a deviation of only 2 - 3° from the previously mentioned crystalline structures, with $[Mn^{III}Mn^{III}(\mu\text{-}O)(dpaq)_2]^{2+}$ having the largest angle of 179°. With these similarities in mind, we determined that treating $[Mn^{III}Mn^{III}(\mu\text{-}O)(dpaq)_2]^{2+}$ with the level of theory outlined in the methods section results

in a reasonable structure for evaluating the energy of formation from $[Mn^{IV}(O)(dpaq)]^{+}$ and $[Mn^{II}(dpaq)(NCMe)]^{+}$.

Geometries of our DFT-optimized $[Mn^{III}Mn^{III}(\mu\text{-}O)(dpaq^{2Me})_2]^{2+}$ species reveal more drastic changes upon substitution at the 2-position of the quinolinyl unit. A space-filling model of $[Mn^{III}Mn^{III}(\mu\text{-}O)(dpaq^{2Me})_2]^{2+}$ shows that the methyl group on the quinoline moiety of one ligand forces a pyridine ring of the other ligand to sit further away from the center of the dimer (Figure S8). This steric interaction only slightly affects the Mn-O bond distance, as there is only a 0.01 Å difference observed between the two (μ-oxo)dimanganese(III, III) species. Subtle changes are seen in the Mn–N distances with a 0.015 Å elongation of the $Mn–N_{ax}$ bond and 0.002 Å elongation of the average $Mn–N_{eq}$ bond for $[Mn^{III}Mn^{III}(\mu\text{-}O)(dpaq^{2Me})_2]^{2+}$. However, the calculated Mn–O–Mn angle is significantly impacted by the steric contribution of the methyl substituent, as the angle of 167° for $[Mn^{III}Mn^{III}(\mu\text{-}O)(dpaq^{2Me})_2]^{2+}$ shows a large deviation from that of 179° for $[Mn^{III}Mn^{III}(\mu\text{-}O)(dpaq)_2]^{2+}$. The Mn(IV)-oxo species do not exhibit such dramatic differences in structural parameters, with the only notable difference being a slight change in the N_{ax}–Mn–O bond angle from 178° for $[Mn^{IV}(O)(dpaq)]^{+}$ to 176° for $[Mn^{IV}(O)(dpaq^{2Me})]^{+}$.

Upon comparing the energies of formation for the two ligand systems, the formation of $[Mn^{III}Mn^{III}(\mu\text{-}O)(dpaq)_2]^{2+}$ was calculated to be 16 kcal mol^{-1} more favorable than the formation of $[Mn^{III}Mn^{III}(\mu\text{-}O)(dpaq^{2Me})_2]^{2+}$ (Figure 3 and Table S3). Thus, we conclude that the steric bulk of the 2-Me-quinolinyl unit in the $dpaq^{2Me}$ ligand disfavors the comproportionation of a $[Mn^{IV}(O)(dpaq^{2Me})]^{+}$ and $[Mn^{II}(dpaq^{2Me})(NCMe)]^{+}$ species to such an extent that hydrogen atom transfer from solvent to $[Mn^{IV}(O)(dpaq^{2Me})]^{+}$ may become competitive.

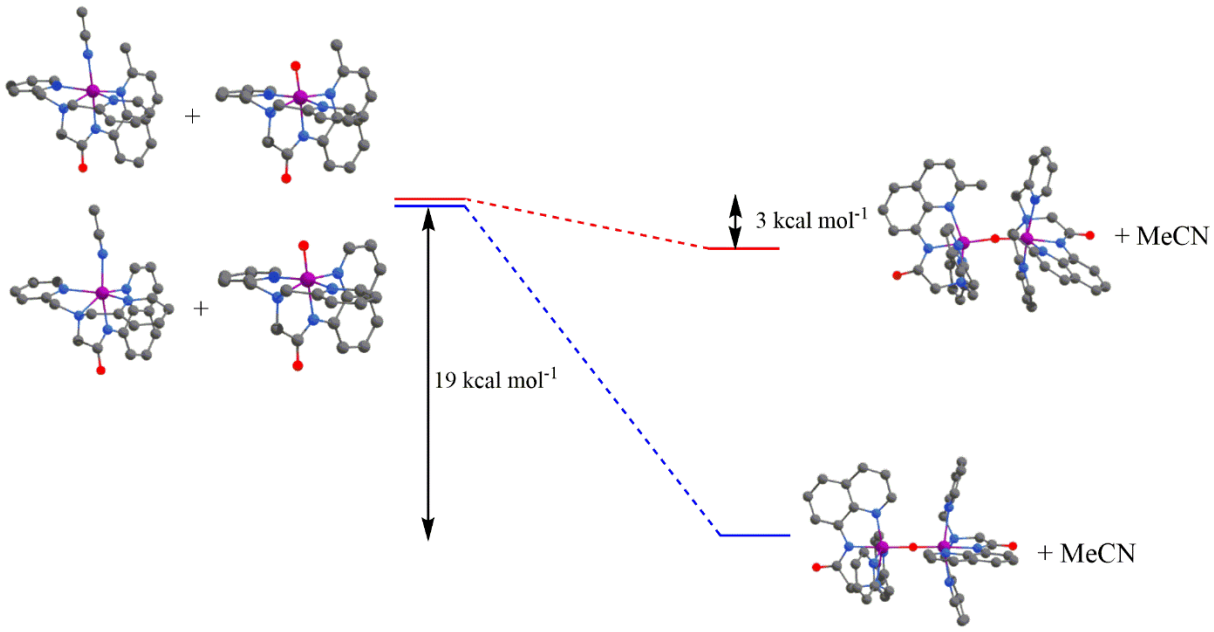

Figure 3. Comparison of the energies of (μ-oxo)dimanganese(III, III) complex formation between the Mn(dpaq) and Mn(dpaq^{2Me}) systems. The formation of $[Mn^{III}Mn^{III}(\mu\text{-}O)(dpaq)_2]^{2+}$ (blue trace) is 16 kcal mol^{-1} more favorable than the formation of $[Mn^{III}Mn^{III}(\mu\text{-}O)(dpaq^{2Me})_2]^{2+}$ (red trace).

Discussion.

Synthetic Mn^{II} systems that are capable of dioxygen activation are relatively rare, and the mechanisms by which these systems operate represent an emerging area of research.[16, 20, 23, 24] Mechanisms of Mn^{II}-based O_2 activation proposed in separate reports are similar in the early steps.[26-31] It is commonly proposed that Mn^{II} complexes bind O_2 to initially form a Mn^{III}-superoxo adduct that is trapped by a second Mn^{II} complex to generate a peroxodimanganese(III, III) species (Scheme 1).[26-28] Each reported mechanism subsequently invokes O−O homolysis, giving either two mononuclear Mn^{IV}-oxo adducts[26, 32] or a bis(μ-oxo)dimanganese(IV, IV) complex (Scheme 1).[21, 31] These high-valent Mn complexes react further to generate Mn^{III} products.[26-31] The system reported by Borovik *et al.* includes a hydrogen-atom transfer step, in which the proposed Mn^{IV}-oxo complex abstracts a hydrogen atom from a solvent molecule to give the Mn^{III}-hydroxo

product.[26] The Kovacs, Lee, and Duboc reports all propose that the Mn^{IV} species (either a mononuclear Mn^{IV}-oxo adduct or a bis(μ-oxo)dimanganese(IV) complex) react with residual Mn^{II} complex in solution to yield (μ-oxo)dimanganese(III, III) products.[27-29, 31] In certain cases, and in the presence of a suitable amount of water, the (μ-oxo)dimanganese(III, III) products can be hydrolyzed to give mononuclear Mn^{III}-hydroxo species.[18, 37]

Steric control of O_2 activation pathways. Our titration experiments investigating the oxygenation of $[Mn^{II}(dpaq)](OTf)$ show that this reaction occurs with a $Mn:O_2$ stoichiometry of 4:1. This result supports a mechanism in which a peroxodimanganese(III, III) dimer undergoes homolytic O−O bond cleavage to yield either a monomeric Mn^{IV}-oxo complex or a bis(μ-oxo)dimanganese(IV) dimer. Either of these species can be sequestered by unreacted $[Mn^{II}(dpaq)]^+$ in solution to form $[Mn^{III}Mn^{III}(\mu\text{-}O)(dpaq)_2]^{2+}$. This dinuclear product has been previously observed and characterized by Mn K-edge X-ray absorption spectroscopy (XAS) and ^1H NMR spectroscopy.[37] In the presence of sufficient concentrations of H_2O, the $[Mn^{III}Mn^{III}(\mu\text{-}O)(dpaq)_2]^{2+}$ species undergoes hydrolysis to result in monomeric $[Mn^{III}(OH)(dpaq)]^+$ (Scheme 3).[37] This mechanism is further supported by the lack of deuterium incorporation observed during the oxygenation of $[Mn^{II}(dpaq)](OTf)$ in d_3-MeCN.

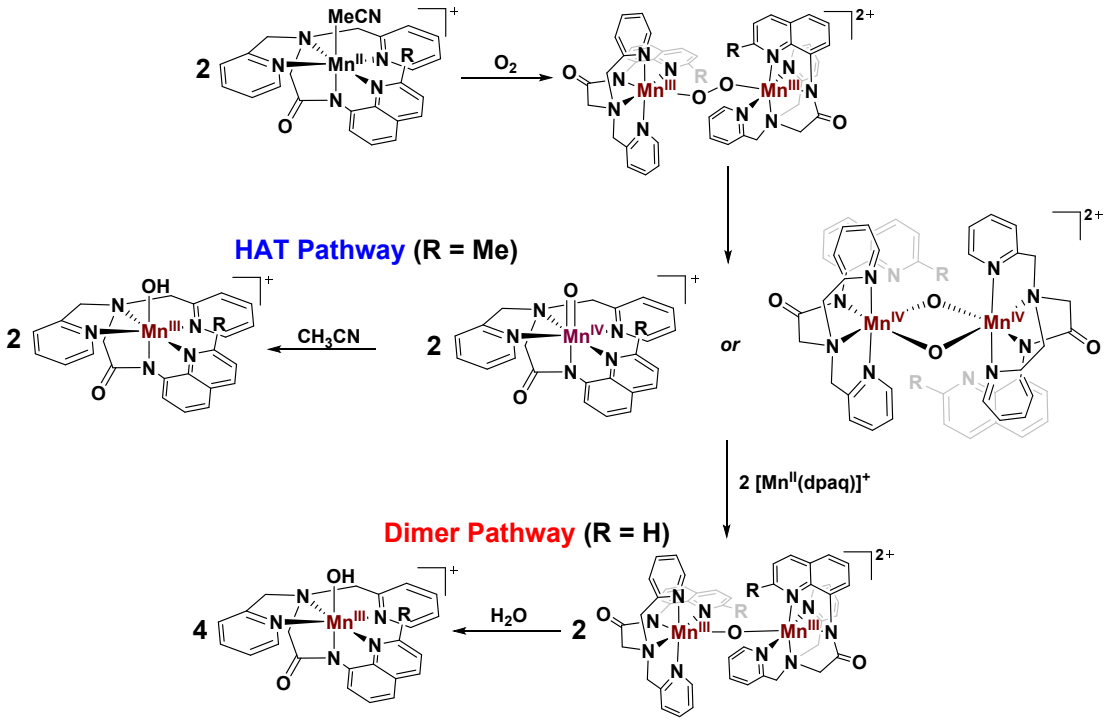

Scheme 3. Proposed pathways for the reactions between $[Mn^{II}dpaq^{R}](OTf)$ with O_2 to generate Mn^{III}-hydroxo species.

The pathway proposed for $[Mn^{II}(dpaq)](OTf)$ is very similar to the mechanism proposed by Kovacs and coworkers for N_4S^- bound Mn^{II} complexes.[27, 29] In that work, the (μ-oxo)dimanganese(III, III) species is proposed to form from the reaction of a Mn^{IV}-oxo intermediate with residual Mn^{II} complex in solution (Scheme 1B).[27, 29] Similarly, a mechanism proposed by Duboc and coworkers suggests that a bis(μ-oxo)dimanganese(IV, IV) species undergoes a series of intramolecular proton transfers and a comproportionation with residual Mn^{II} complex in solution to yield a (μ-hydroxo)dimanganese(III, III) species (Scheme 1C).[28, 30] In a system without acidic protons available from the ligand, one can envision a pathway along which the bis(μ-oxo)dimanganese(IV, IV) intermediate reacts with residual Mn^{II} complex in solution to form a (μ-oxo)dimanganese(III, III) species (Scheme 4). Such a mechanism has been proposed for the reaction of Mn^{II}(SALPRN) with O_2 (SALPRN = 1,3-bis(salicylideneamino)propane).[65]

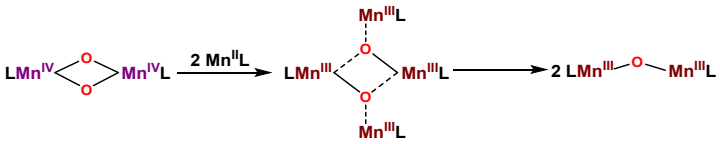

Scheme 4. A bis(μ-oxo)dimanganese(IV, IV) dimer could react with Mn^{II} complex in solution to form a (μ-oxo)dimanganese(III, III) species through a tetranuclear intermediate.

O_2 titration experiments for the bulkier $[Mn^{II}(dpaq^{2Me})](OTf)$ complex show that dioxygen activation proceeds with a 2:1 Mn:O_2 stoichiometry, and deuterium incorporation is observed in a deuterated solvent. Compared to $[Mn^{II}(dpaq)](OTf)$, these results suggest a divergent mechanism in which a Mn^{IV}-oxo intermediate (either a terminal oxo or a bis(μ-oxo)dimanganese(IV, IV) species) abstracts a hydrogen-atom from solvent (Scheme 3).

Our computational investigations show that the formation of $[Mn^{III}Mn^{III}(\mu\text{-}O)(dpaq^{2Me})_2]^{2+}$ from a Mn^{IV}-oxo complex and Mn^{II} complex is ca. 16 kcal mol^{-1} less favorable than the analogous formation of $[Mn^{III}Mn^{III}(\mu\text{-}O)(dpaq)_2]^{2+}$ (Figure 3). This large change supports the lack of dinuclear products observed by ^1H NMR and XAS experiments upon dissolution of the $[Mn^{III}(OH)(dpaq^{2Me})](OTf)$ complex.[37] $[Mn^{II}(dpaq^{2Me})](OTf)$ stands in contrast to the majority of Mn^{II} systems that activate dioxygen and form Mn^{III}-hydroxo complexes, only sharing a mechanism with $[Mn(1^{cyp})]^-$ (1^{cyp} = tris(N-cyclopentylcarbamoylmethyl)amine).[26-29, 31] This latter complex also contains bulky substituents near the expected site of O_2 binding and activation.

Mononuclear Oxomanganese(IV) versus dinuclear bis(μ-oxo)dimanganese(IV, IV) intermediates. The formation of $[Mn^{III}(OD)(dpaq^{2Me})]^+$ from oxygenation of $[Mn^{II}(dpaq^{2Me})](OTf)$ in d_3-MeCN is consistent with hydrogen-atom abstraction from solvent by a high-valent oxomanganese(IV) intermediate. Our proposed mechanism for O_2 activation for $[Mn^{II}(dpaq)](OTf)$ also requires the formation of an oxomanganese(IV) intermediate (Scheme 3). In either system, it is unclear whether the proposed high-valent intermediate is a mononuclear

Mn^{IV}-oxo adduct or a bis(μ-oxo)dimanganese(IV, IV) species. The formation of a bis(μ-oxo)dimanganese(IV, IV) intermediate would likely require the dissociation of an arm of the $dpaq^R$ ligand to retain hexacoordination at the Mn center (Scheme 3). Thus, in the hypothetical $[Mn^{IV}Mn^{IV}(\mu\text{-oxo})_2(dpaq^R)_2]^{2+}$ species, the $dpaq^R$ ligand would be bound in a tetradentate (κ^4) fashion, rather than the commonly observed pentadentate (κ^5) mode. The κ^4 binding of potentially pentadentate ligands has been observed in the XRD structures of dimanganese complexes with two bridging oxo ligands. Specifically, the XRD structures of $[Mn^{III}Mn^{IV}(\mu\text{-O})_2(N4Py)_2]^{3+}$, $[Mn^{IV}Mn^{IV}(\mu\text{-O})_2(bpmg)_2](ClO_4)_2$, and $[Mn^{IV}Mn^{IV}(\mu\text{-O})_2(mcbpen)_2](ClO_4)_2$ each show nominally pentadentate ligand bound in a κ^4 mode with non-coordinated pyridine moiety (N4Py = *N,N*-bis(2-pyridylmethyl)-*N*-bis(2-pyridyl)methylamine, bpmg = d 2-[[2-[bis(pyridin-2-ylmethyl)amino]-ethyl](methyl)amino]acetic acid, mcbpen = N-methyl-N0 - carboxymethyl-N,N0 - bis(pyridylmethyl)ethane-1,2-diamine).[66, 67] Tetradentate binding of the dpaq ligand has been previously proposed for the $[Mn^{III}Mn^{IV}(\mu\text{-O})(dpaq)_2]^{3+}$ complex, which was generated from the reaction between $[Mn^{III}(OH)(dpaq)]^+$ and H_2O_2.[68] Although a crystal structure of this bis(μ-oxo)dimanganese(III, IV) complex was not reported, a DFT-optimized structure showed a non-coordinated quinoline moiety.[68] The reaction of $[Mn^{III}Mn^{IV}(\mu\text{-O})(dpaq)_2]^{3+}$ with phenolic substrates generated the monomeric $[Mn^{III}(OH)(dpaq)]^+$ complex in quantitative yield, where the dpaq ligand is again pentadentate.[68] These results suggest that the dpaq ligand can alternate between pentadentate and tetradentate binding modes without decordinating fully from the Mn center. This flexibility could allow for the formation of bis(μ-oxo)dimanganese(III, IV) intermediate en route to (μ-oxo)dimanganese(III, III) or hydroxomanganese(III) products (Scheme 3).

Alternatively, a terminal Mn^{IV}-oxo adduct could serve as the high-valent intermediate formed during oxygenation of $[Mn^{II}(dpaq)](OTf)$ and $[Mn^{II}(dpaq^{2Me})](OTf)$. A recent report has proposed that iodosylbenzene oxidation of $[Mn^{III}(OH)(dpaq)]^+$ in the presence of the redox-inactive Lewis acid salts (such as $Sc(OTf)_3$) results in the formation of Mn^{IV}-oxo – Lewis acid adducts.[69] EPR experiments provided evidence for the Mn^{IV} oxidation state. The Mn^{IV}-oxo – Lewis acid adducts were capable of reacting with substrates with weak C–H bonds. Oxygenation of $[Mn^{II}(dpaq^{2Me})](OTf)$ appears to result in the oxidation of the strong C–H of acetonitrile (C–H bond dissociation energy of ~94 kcal mol^{-1}).[70] Given that the coordination of Lewis acids to Mn^{IV}-oxo species can suppress reactivity towards C–H bonds, a $[Mn^{IV}(O)(dpaq^{2Me})]^+$ species formed in the absence of Lewis acids could be a strong oxidant. However, when the oxygenation of $[Mn^{II}(dpaq^{2Me})]^+$ was performed in the presence of substrates with C–H bonds weaker than that of MeCN (such as ethylbenzene and toluene, which have bond dissociation energies of ~86 and ~92 kcal mol^{-1}, respectively),[71, 72] no substrate oxidation was observed. The reason for the lack of substrate oxidation under these conditions is unclear at present. It could be that the large excess of MeCN relative to substrate favors oxidation of the former. Alternatively, if a bis(μ-oxo)dimanganese(IV, IV) intermediate is responsible for abstracting a hydrogen atom from MeCN, the expected steric bulk of this high-valent species could hinder the approach of substrates more sterically bulky than the relatively small MeCN molecule.

Conclusions.

Inspired by the dioxygen activating ability of some of Nature's Mn-containing metalloenzymes, there has been interest in developing Mn-based synthetic catalysts that can employ O_2 for the oxidation of organic substrates. However, there are relatively few synthetic Mn^{II}

complexes that are capable of dioxygen activation, and details regarding their mechanistic pathways are limited. In an effort to garner further mechanistic understanding of O_2-activation processes of Mn^{II} center, this report investigates two monomeric Mn^{II} complexes supported by pentadentate ligands that have been previously reported to react with O_2 to produce monomeric Mn^{III}-hydroxo species.[36, 73] One of the complexes, [Mn^{II}dpaq](OTf), activates dioxygen by a 4:1 Mn:O_2 stoichiometry. This stoichiometry suggests a mechanism in which a (μ-oxo)dimanganese(III, III) dimer is formed through the comproportionation of a Mn^{IV}-oxo species (either a terminal Mn-oxo or a bis(μ-oxo)dimanganese(IV, IV) dimer) and residual Mn^{II} complex in solution. This proposed comproportionation mechanism joins the majority of preceding systems described to form Mn^{III}-hydroxo complexes by O_2 oxidation of Mn^{II} precursors.[27-32] In contrast, the bulkier [Mn^{II}dpaq^{2Me}](OTf) complex operates according to a 2:1 Mn:O_2 stoichiometry, suggesting a mechanism where a terminal Mn^{IV}-oxo species abstracts a hydrogen atoms from solvent. In support, oxygenation of [Mn^{II}(dpaq^{2Me})](OTf) in deuterated MeCN resulted in Mn^{III}–OD formation. The only other system for which a dioxygen activation mechanism involving hydrogen-atom abstraction from solvent was reported also employed a sterically-encumbered ligand.[26] Thus, simple steric modification of ligands may be an important approach to generate reactive, high-valent Mn species through O_2 activation.

Conflicts of interest. The authors declare no conflict of interest.

Acknowledgements. This work was supported by the U.S. Department of Energy (DE-SC0016359). Support for the NMR instrumentation was provided by NIH Shared Instrumentation Grant # S10OD016360.

References.

1. A. J. Jasniewski and L. Que, *Chem. Rev.*, 2018, **118**, 2554-2592.
2. X. Huang and J. T. Groves, *Chem. Rev.*, 2018, **118**, 2491-2553.
3. A. T. Fiedler and A. A. Fischer, *J. Biol. Inorg. Chem.*, 2017, **22**, 407-424.
4. E. I. Solomon, D. E. Heppner, E. M. Johnston, J. W. Ginsbach, J. Cirera, M. Qayyum, M. T. Kieber-Emmons, C. H. Kjaergaard, R. G. Hadt and L. Tian, *Chem. Rev.*, 2014, **114**, 3659-3853.
5. K. D. E. Koehntop, J. P.; Que, L., Jr., *J. Biol. Inorg. Chem.*, 2005, **10**, 87-93.
6. W. A. Gunderson, A. I. Zatsman, J. P. Emerson, E. R. Farquhar, L. Que, J. D. Lipscomb and M. P. Hendrich, *J. Am. Chem. Soc.*, 2008, **130**, 14465-14467.
7. M. H. K. Glickman, J. P., *Biochemistry*, 1995, 14077-14092.
8. C. S. Su, M.; Oliw, E. H., *J. Biol. Chem.*, 2000, 18830-18835.
9. A. Wennman, S. Karkehabadi and E. H. Oliw, *Arch. Biochem. Biophys.*, 2014, **555-556**, 9-15.
10. O. Opaleye, R.-S. Rose, M. M. Whittaker, E.-J. Woo, J. W. Whittaker and R. W. Pickersgill, *J. Biol. Chem.*, 2006, **281**, 6428-6433.
11. T. Borowski, A. Bassan, N. G. J. Richards and P. E. M. Siegbahn, *J. Chem. Theory Comp.*, 2005, **1**, 686-693.
12. A. Tanner, L. Bowater, S. A. Fairhurst and S. Bornemann, *J. Biol. Chem.*, 2001, **276**, 43627-43634.
13. L. C. G. Tabares, J.; Hureau, C.; Burell, M. R.; Bowater, L.; Pecoraro, V. L.; Bornemann, S.; Un, S., *J. Phys. Chem. B.*, 2009, **113**, 9016-9025.
14. P. d. B. Saisaha, J. W.; Browne, W. R., *Chem. Soc. Rev.*, 2013, **42**, 2059-2074.
15. E. V. Rybak-Akimova, in *Physical Inorganic Chemistry*, ed. A. Bakac, John Wiley and Sons, Inc., Hoboken, NJ, 2010, ch. Mechanisms of Oxygen Binding and Activation at Transition Metal Centers., pp. 109-188.
16. V. L. Pecoraro, M. J. Baldwin and A. Gelasco, *Chem. Rev.*, 1994, **94**, 807-826.
17. R. L. Shook, S. M. Peterson, J. Greaves, C. Moore, A. L. Rheingold and A. S. Borovik, *J. Am. Chem. Soc.*, 2011, **133**, 5810-5817.
18. M. K. B. Coggins, L. M.; Kovacs, J. M., *Inorg. Chem.*, 2013, **52**, 12383-12393.
19. G. C. Wijeratne, B.; Day, V. W.; Jackson, T. A., *Inorg. Chem.*, 2014, **53**, 7622-7634.
20. P. Battioni, J. F. Bartoli, P. Leduc, M. Fontecave and D. Mansuy, *Chem. Comm.*, 1987, 791-792.
21. C. P. Horwitz, S. E. Creager and R. W. Murray, *Inorg. Chem.*, 1990, **29**, 1006-1011.
22. C. Zhang, Z. Xu, T. Shen, G. Wu, L. Zhang and N. Jiao, *Org. Lett.*, 2012, **14**, 2362-2365.
23. J. Christoffers, *The Journal of Organic Chemistry*, 1999, **64**, 7668-7669.
24. Y. Nishida, N. Tanaka, A. Yamazaki, T. Tokii, N. Hashimoto, K. Ide and K. Iwasawa, *Inorg. Chem.*, 1995, **34**, 3616-3620.
25. H. Komatsuzaki, Y. Nagasu, K. Suzuki, T. Shibasaki, M. Satoh, F. Ebina, S. Hikichi, M. Akita and Y. Moro-oka, *J. Chem. Soc., Dalton Trans.*, 1998, 511-512.
26. Z. Shirin, A. S. Borovik and V. G. Young Jr, *Chem. Comm.*, 1997, 1967-1968.
27. M. K. Coggins, X. Sun, Y. Kwak, E. I. Solomon, E. Rybak-Akimova and J. A. Kovacs, *J. Am. Chem. Soc.*, 2013, **135**, 5631-5640.

28. D. C. R. Brazzolotto, Fabian G.; Smith-Jones, Julian; Retegan, Marius; Amidani, Lucia; Faponle, Abayomi S.; Ray, Kallol; Philouze, Christian; de Visser, Sam P.; Gennari, Marcello; Duboc, Carole, *Angew. Chem.*, 2017, **56**, 8211-8215.
29. M. K. Coggins, S. Toledo, E. Shaffer, W. Kaminsky, J. Shearer and J. A. Kovacs, *Inorg. Chem.*, 2012, **51**, 6633-6644.
30. M. B. Gennari, Deborah; Pecaut, Jacques; Cherrier, Mickael V.; Pollock, Christopher J.; DeBeer, Serena; Retegan, Marius; Pantazis, Dimitrios A.; Neese, Frank; Rouzieres, Mathieu; Clerac, Rodolphe; Duboc, Carole, *J. Am. Chem. Soc.*, 2015, **137**, 8644-8653.
31. W.-Y. W. Chien-Ming Lee, Ming-Hsi Chiang, D. Scott Bohle, Gene-Hsiang Lee, *Inorg. Chem.*, 2017, **56**, 10559-10569.
32. J. A. Rees, V. Martin-Diaconescu, J. A. Kovacs and S. DeBeer, *Inorg. Chem.*, 2015, **54**, 6410-6422.
33. C.-M. Lee, C.-H. Chuo, C.-H. Chen, C.-C. Hu, M.-H. Chiang, Y.-J. Tseng, C.-H. Hu and G.-H. Lee, *Angew. Chem. Int. Ed.*, 2012, **51**, 5427-5430.
34. D. B. Rice, A. A. Massie and T. A. Jackson, *Acc. Chem. Res.*, 2017, **50**, 2706-2717.
35. D. F. Leto and T. A. Jackson, *J. Biol. Inorg. Chem.*, 2014, **19**, 1-15.
36. D. B. W. Rice, Gayan B.; Burr, Andrew D.; Parham, Joshua D.; Day, Victor W.; Jackson, Timothy A., *Inorg. Chem.*, 2016, **55**, 8110-8120.
37. D. B. Rice, S. D. Jones, J. T. Douglas and T. A. Jackson, *Inorg. Chem.*, 2018, **57**, 7825-7837.
38. D. B. Rice, A. Munasinghe, E. N. Grotemeyer, A. D. Burr, V. W. Day and T. A. Jackson, *Inorg. Chem.*, 2019, **58**, 622-636.
39. C. L. Achord J. M.; Hussey, *Anal. Chem.*, 1980, **52**, 601-602.
40. A. D. Becke, *J. Chem. Phys.*, 1986, **84**, 4524-4529.
41. J. P. Perdew, *Phys. Rev. B*, 1986, **33**, 8822-8824.
42. F. Neese, *J. Comput. Chem.*, 2003, **24**, 1740-1747.
43. F. Neese, *Wiley Interdisciplinary Reviews: Computational Molecular Science*, 2018, **8**, e1327.
44. A. D. Becke, *J. Chem. Phys.*, 1993, **98**, 1372-1377.
45. A. D. Becke, *J. Chem. Phys.*, 1993, **98**, 5648-5652.
46. C. Lee, W. Yang and R. G. Parr, *Phys. Rev. B*, 1988, **37**, 785-789.
47. R. Izsák and F. Neese, *J. Chem. Phys.*, 2011, **135**, 144105.
48. F. Neese, F. Wennmohs, A. Hansen and U. Becker, *Chem. Phys.*, 2009, **356**, 98-109.
49. F. Weigend and R. Ahlrichs, *PCCP*, 2005, **7**, 3297-3305.
50. A. Schäfer, H. Horn and R. Ahlrichs, *J. Chem. Phys.*, 1992, **97**, 2571-2577.
51. A. Schäfer, C. Huber and R. Ahlrichs, *J. Chem. Phys.*, 1994, **100**, 5829-5835.
52. L. Noodleman, *J. Chem. Phys.*, 1981, **74**, 5737-5743.
53. L. Noodleman and E. R. Davidson, *Chem. Phys.*, 1986, **109**, 131-143.
54. R. Caballol, O. Castell, F. Illas, I. de P. R. Moreira and J. P. Malrieu, *J. Phys. Chem. A*, 1997, **101**, 7860-7866.
55. V. Barone and M. Cossi, *J. Phys. Chem. A*, 1998, **102**, 1995-2001.
56. M. Cossi, N. Rega, G. Scalmani and V. Barone, *J. Comput. Chem.*, 2003, **24**, 669-681.
57. A. M. D. Massie, Melissa C.; Cardoso. Luisa T.; Walker, Ashlie M.; Hossain, M. Kamal; Day, Victor W.; Nordlander, Ebbe; Jackson, Timothy A., *Angew. Chem. Int. Ed.*, 2017, **56**, 4178-4182.

58. A. A. Massie, A. Sinha, J. D. Parham, E. Nordlander and T. A. Jackson, *Inorg. Chem.*, 2018, **57**, 8253-8263.
59. M. C. Denler, A. A. Massie, R. Singh, E. Stewart-Jones, A. Sinha, V. W. Day, E. Nordlander and T. A. Jackson, *Dalton Trans.*, 2019, **48**, 5007-5021.
60. I. Garcia-Bosch, A. Company, C. W. Cady, S. Styring, W. R. Browne, X. Ribas and M. Costas, *Angew. Chem. Int. Ed.*, 2011, **50**, 5648-5653.
61. D. F. Leto, R. Ingram, V. W. Day and T. A. Jackson, *Chem. Comm.*, 2013, **49**, 5378-5380.
62. D. F. Leto, A. A. Massie, D. B. Rice and T. A. Jackson, *J. Am. Chem. Soc.*, 2016, **138**, 15413-15424.
63. T. H. Parsell, M.-Y. Yang and A. S. Borovik, *J. Am. Chem. Soc.*, 2009, **131**, 2762-2763.
64. K.-B. Cho, S. Shaik and W. Nam, *J. Phys. Chem. Let.*, 2012, **3**, 2851-2856.
65. P. J. W. Colin P. Horwitz, Joseph T. Warden, and Carol A. Lisek, *Inorg. Chem.*, 1993, **32**, 82-88.
66. D. F. Leto, S. Chattopadhyay, V. W. Day and T. A. Jackson, *Dalton Trans.*, 2013, **42**, 13014.
67. G. Berggren, A. Thapper, P. Huang, L. Eriksson, S. Styring and M. F. Anderlund, *Inorg. Chem.*, 2011, **50**, 3425-3430.
68. M. Sankaralingam, S. H. Jeon, Y.-M. Lee, M. S. Seo, K. Ohkubo, S. Fukuzumi and W. Nam, *Dalton Trans.*, 2016, **45**, 376-383.
69. M. Sankaralingam, Y.-M. Lee, Y. Pineda-Galvan, D. G. Karmalkar, M. S. Seo, S. H. Jeon, Y. Pushkar, S. Fukuzumi and W. Nam, *J. Am. Chem. Soc.*, 2019, **141**, 1324-1336.
70. D. J. Goebbert, L. Velarde, D. Khuseynov and A. Sanov, *J. Phys. Chem. Let.*, 2010, **1**, 792-795.
71. J. J. Warren, T. A. Tronic and J. M. Mayer, *Chem. Rev.*, 2010, **110**, 6961-7001.
72. Y. R. Luo, in *Comprehensive Handbook of Chemical Bond Energies.*, CRC Press, 2007, pp. 19-145.
73. G. B. Wijeratne, B. Corzine, V. W. Day and T. A. Jackson, *Inorg. Chem.*, 2014, **53**, 7622-7634.

Table of Contents Synopsis.

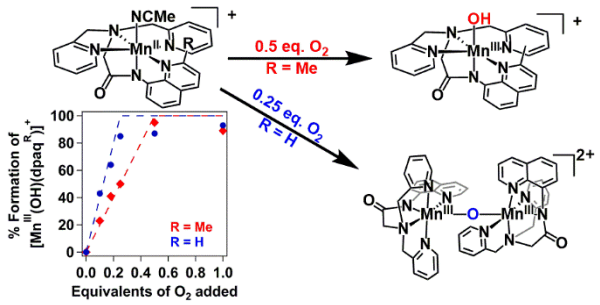

Steric control of dioxygen activation is demonstrated through O_2 titration and isotopic labeling experiments for two Mn(II) complexes.